Available online at www.sciencedirect.com

ScienceDirect

Geochimica et Cosmochimica Acta 208 (2017) 185–197

Geochimica et Cosmochimica Acta

www.elsevier.com/locate/gca

Concentration effect on equilibrium fractionation of Mg-Ca isotopes in carbonate minerals: Insights from first-principles calculations

Wenzhong Wang [a,b], Tian Qin [a,b], Chen Zhou [c], Shichun Huang [d], Zhongqing Wu [a,b,*], Fang Huang [c,*]

[a] *Laboratory of Seismology and Physics of Earth's Interior, School of Earth and Space Sciences, University of Science and Technology of China, Hefei, Anhui 230026, China*

[b] *Mengcheng National Geophysical Observatory, Anhui, China*

[c] *CAS Key Laboratory of Crust-Mantle Materials and Environments, School of Earth and Space Sciences, University of Science and Technology of China, Hefei, Anhui 230026, China*

[d] *Department of Geoscience, University of Nevada, Las Vegas, NV 89154, United States*

Received 20 October 2016; accepted in revised form 21 March 2017; Available online 29 March 2017

Abstract

Naturally occurring carbonates have a wide variation in Mg and Ca contents. Using the density-functional-theory calculations, this study examines the effect of Mg and Ca concentrations on bond lengths and equilibrium fractionation factors of Mg-Ca isotopes among calcite-type carbonate minerals ($Mg_xCa_{1-x}CO_3$). Mg content x and Ca content $(1-x)$ of the investigated carbonate minerals range from 1/12 to 1 and from 1/36 to 1, respectively. Concentration of Ca and Mg in carbonates have significant effects on Ca–O and Mg–O bond lengths when x is close to 0, 0.5 or 1. Because equilibrium isotope fractionation factors ($10^3\ln\alpha$) are mainly controlled by their relevant bond strengths, which can be measured using their average bond lengths, $10^3\ln\alpha$ of $^{26}Mg/^{24}Mg$ and $^{44}Ca/^{40}Ca$ between calcite-type carbonate minerals and dolomite also vary dramatically with Mg content, especially when x is close to 0 and 1. For instance, at 300 K, $10^3\ln\alpha$ of $^{26}Mg/^{24}Mg$ between $Mg_{1/12}Ca_{11/12}CO_3$ and dolomite ($x = 0.5$) is $\sim -4.3‰$, while $10^3\ln\alpha$ of $^{44}Ca/^{40}Ca$ between $Mg_{23/24}Ca_{1/24}CO_3$ and dolomite is $\sim 6‰$. Dolomite is enriched in ^{26}Mg but depleted in ^{44}Ca relative to all other carbonate minerals, which is consistent with it having the shortest Mg–O bond length and the longest Ca–O bond lengths among all carbonates. At 300 K, a small change of x from 0.5 to 0.6 in dolomite could result in 1‰ variation in $10^3\ln\beta$ of $^{26}Mg/^{24}Mg$. Therefore, the concentration effect in carbonate minerals should be taken into account when applying the isotope fractionation factors of carbonate minerals to understand geochemical processes.

Keywords: First-principle calculations; Concentration effect; Equilibrium fractionation; Mg-Ca isotopes; Carbonates

1. INTRODUCTION

Carbonates are important components of sediments, recording many fundamental environmental and geochemical processes. Calcite, dolomite, and magnesite are the major carbonate minerals in sedimentary rocks. C, O, Mg, and Ca stable isotopic compositions of these carbon-

* Corresponding authors at: Laboratory of Seismology and Physics of Earth's Interior, School of Earth and Space Sciences, University of Science and Technology of China, Hefei, Anhui 230026, China (Z. Wu).

E-mail addresses: wuzq10@ustc.edu.cn (Z. Wu), fhuang@ustc.edu.cn (F. Huang).

http://dx.doi.org/10.1016/j.gca.2017.03.023

ates have a number of essential implications. For example, the oxygen isotopic compositions in carbonate minerals have been used as a thermometry investigating paleo-climate change (e.g., Kim and O'Neil, 1997; Bemis et al., 1998; McDermott, 2004; Lea, 2014). Carbon isotope excursions in marine carbonates and sedimentary organic matters are often related to catastrophic events in the Earth's history (e.g., Kaufman and Knoll, 1995; Hoffman et al., 1998; Shields-Zhou and Och, 2011; Johnston et al., 2012; Sahoo et al., 2012), and they are the key parameters in the study of carbon cycling and paleo-climate changes (Werne and Hollander, 2004; Ader et al., 2009; Meyer et al., 2013).

More recently, Ca isotopic compositions in marine carbonates have been used to constrain global Ca cycling (De La Rocha, 2000; Heuser et al., 2005; Farkaš et al., 2007), and Mg isotope data in carbonates have been applied to constrain the oceanic cycling of Mg and continental weathering (Tipper et al., 2006b; Higgins and Schrag, 2010; Li et al., 2015). Furthermore, since Mg and Ca fluxes are usually coupled with carbon cycles, Mg-Ca isotopes have great potential to trace deep carbon recycling (DePaolo, 2004; Huang et al., 2011, 2015; Yang et al., 2012; Zhang and Li, 2012; Cheng et al., 2015; Liu et al., 2015). Reported $\delta^{26/24}$Mg values of precipitated marine carbonates vary from around −5‰ to −1‰ in magnesian calcites (Galy et al., 2002; de Villiers et al., 2005; Tipper et al., 2006a,b; Buhl et al., 2007; Hippler et al., 2009), and from ∼−2‰ to −1‰ in dolomites (Galy et al., 2002; Chang et al., 2003; Jacobson et al., 2010). It is not clear whether the $\delta^{26/24}$Mg variations in carbonate minerals reflect different precipitation environments or Mg isotopic fractionation among Mg-bearing species. Therefore, in order to better apply stable isotope data into geochemical studies, it is critical to understand equilibrium isotope fractionation factors among carbonate minerals.

Chemical compositions of carbonate minerals vary tremendously as solid solutions due to the incorporations of divalent cations including Mg^{2+}, Sr^{2+}, Ba^{2+}, and Cd^{2+} (Tesoriero and Pankow, 1996; Huang and Fairchild, 2001). Generally, Mg^{2+} cations could substitute Ca^{2+} cations to form low-Mg calcite (with <4 mol% Mg, mole ratio hereafter defined as Mg/(Mg + Ca)) and high-Mg calcite (with >4 mol% Mg). The Mg content of experimentally synthesized calcites in aqueous solutions could be up to 22 mol% (Mucci and Morse, 1983; Mucci, 1986; Huang and Fairchild, 2001; Meldrum and Hyde, 2001; Li et al., 2012), but magnesites with low Ca content were rarely reported in literature. Although naturally occurring dolomites generally contain 50 mol% $MgCO_3$ in an idealized mineral structure, they also show variable Mg contents (about 40–50 mol%) (Drits et al., 2005).

Variations of the chemical compositions may affect structures of minerals, which further impacts the equilibrium isotope fractionation factors among minerals. For example, based on first-principles calculations, Feng et al. (2014) reported that equilibrium Ca isotope fractionation factors between clinopyroxene (cpx) and orthopyroxene (opx) are controlled not only by temperature, but also the Ca content in opx. Pinilla et al. (2015) reported the noticeable equilibrium Mg isotopes fractionation between Mg-calcites with Mg contents of 3.12 mol% and 6.25 mol%. However, their calculations were conducted with the fixed cell parameters, which means that these two investigated Mg-calcites may not be under the same pressure and thus they are not in thermodynamic equilibrium. It is therefore important to scrutinize the possible concentration effect on stable isotope fractionation among carbonate minerals.

It is challenging to synthesize carbonate minerals with a wide range of controllable Mg contents at ambient conditions through inorganic experiments, and synthesis of dolomite is even referred to as the "dolomite problem" for decades (Zenger et al., 1980; Land, 1998; Warren, 2000). Therefore, experimental determination of the equilibrium isotopes fractionation between carbonate minerals with variable chemical compositions remains a great challenge. No experimental study has yet been reported to examine the concentration effect on the equilibrium isotope fractionation between carbonate minerals. Mg isotope fractionation factors between carbonate minerals (Mg-calcite and dolomite) and aqueous Mg solutions were experimentally measured at various temperatures (Pearce et al., 2012; Li et al., 2012, 2015; Saulnier et al., 2012; Mavromatis et al., 2013) and theoretically calculated (Rustad et al., 2010; Schauble, 2011), but there is a significant discrepancy between experimental and theoretical results. This highlights the complexity of determining isotope fractionation factors, such as kinetic effect (Saenger and Wang, 2014). The Mg concentration variations in synthesized carbonate minerals may also contribute to the complexity.

Recent advances in computational capabilities prove that the density functional theory (DFT) provides a powerful tool to calculate equilibrium isotope fractionation factors. DFT calculations, which show comparable precision relative to the well-designed experiments (Lejaeghere et al., 2016), have been widely used to calculate equilibrium fractionation factors for a number of systems such as Mg, Si, Ca, and V (Schauble et al., 2004; Griffith et al., 2008; Méheut et al., 2009; Schauble, 2011; Li and Liu, 2011; Kowalski and Jahn, 2011; Kowalski et al., 2013; Huang et al., 2013, 2014; Feng et al., 2014; Wu et al., 2015). Natural calcite and magnesite are solid solutions with substantial variations in Ca-Mg concentration. For better understanding the concentration effect on equilibrium isotope fractionation, we estimate fractionation factors of Mg and Ca isotopes among carbonate minerals ($Mg_xCa_{1-x}CO_3$) with x varying from 0 to 1 using the DFT calculations. We focus on the effect of Ca-Mg substitutions on carbonate mineral structures, Ca–O and Mg–O bonding, and equilibrium isotope fractionation. Our results reveal a significant concentration effect on equilibrium fractionation of Mg-Ca isotopes in carbonate minerals.

2. CALCULATION METHODS

Equilibrium isotope fractionation arises from changes in vibrational frequencies caused by isotopic substitution of an interested element in two phases (Bigeleisen and Mayer, 1947; Urey, 1947). The isotope fractionation factor of element X between two phases A and B, α_{A-B}, is the ratio

of their isotope ratios of these two phases under equilibrium. According to Richet et al. (1977), the isotope fractionation factor between Phase A and an ideal gas of X atoms is the reduced partition function ratio β_A of the Element X, defined in the harmonic approximation as:

$$\beta_A = \frac{Q_h}{Q_l} = \prod_i^{3N} \frac{u_{ih}}{u_{il}} \frac{e^{-\frac{1}{2}u_{ih}}}{1-e^{-u_{ih}}} \frac{1-e^{-u_{il}}}{e^{-\frac{1}{2}u_{il}}} \quad (1)$$

where Q is the vibrational partition function, index h and l refer to the heavy and light isotopes, respectively; i is a running index of vibrational frequency mode, and N is the number of atoms in the unit cell. A crystal with N atoms has $3N$ vibrational modes and the product runs over all $3N$ phonon modes. u_{ih} and u_{il} are defined as:

$$u_{ih\ or\ il} = h\omega_{ih\ or\ il}/k_B T \quad (2)$$

where h is the Planck constant, k_B is the Boltzmann constant, T is temperature in Kelvin, and $\omega_{ih\ or\ il}$ is the vibrational frequency of the i^{th} mode. Following Richet et al. (1977), the equilibrium isotope fractionation between two Phases A and B can be rewritten in per mil as:

$$\Delta_{A-B} = 10^3 \ln \alpha_{A-B} = 10^3 \ln \beta_A - 10^3 \ln \beta_B \quad (3)$$

The calculation details in this study are similar to that published in previous work (Schauble, 2011; Li and Liu, 2011; Huang et al., 2013, 2014; Feng et al., 2014; Wu et al., 2015). All calculations were performed using an open-source software "Quantum Espresso" based on the DFT, plane wave, and pseudopotential (Giannozzi et al., 2009). Electronic wave functions are expanded by a plane-wave basis set. The interaction between the valence electrons and the ionic core is described using pseudopotential. Local density approximation (LDA) for exchange correlation functional (Perdew and Zunger, 1981) was used in this study because of its advantages on calculating mineral structures and thermodynamic properties of minerals (Wentzcovitch et al., 2010; Huang et al., 2013). The plane-wave cutoff energy is 70 Ry.

The pseudopotentials of calcium and carbon were generated using Vanderbilt method (Vanderbilt, 1990) with a configuration of $3s^2 3p^6 4s^1$ and a 1.85 Bohr cutoff radius for calcium, and a configuration of $2s^2 2p^2$ and a 1.3 Bohr cutoff radius for carbon. The pseudopotential of magnesium was generated using the method of von Barth and Car for all channels using a 2.5 Bohr cutoff radius and five configurations, $3s^2 3p^0$, $3s^1 3p^1$, $3s^1 3p^{0.5} 3d^{0.5}$, $3s^1 3p^{0.5}$, $3s^1 3d^1$, with weights of 1.5, 0.6, 0.3, 0.3, 0.2, respectively. The oxygen pseudopotential was generated by the method of Troullier and Martins (1991) with configuration $2s^2 2p^4$ and a cutoff radius of 1.45 Bohr. Brillouin zone integrations over electronic states were performed with $N_1 \times N_2 \times N_3$ k-point grid dependent on the size of unit cells (see Table S1).

The initial calcite crystal structures were obtained from previous experimental studies (Graf, 1961; Markgraf and Reeder, 1985). Crystal structures with variable Mg contents were well optimized using variable cell shape molecular dynamics (Wentzcovitch, 1991) and the residual forces converge within 10^{-4} Ry/Bohr. The dynamical matrices were calculated on a regular q mesh dependent on the size of unit cells (Table S1) using the density-functional perturbation theory (DFPT) and then interpolated on a dense q mesh to obtain the vibrational density of the state of minerals.

3. RESULTS

3.1. Relaxed crystal structures

The unit structure cell of calcite with space group R-3c contains six symmetry-equivalent Ca atoms (Graf, 1961; Markgraf and Reeder, 1985). All initial carbonate structures before optimization, with Mg/(Mg + Ca) (mole ratio hereafter) varying from 1/12 to 1, were obtained by replacing Ca atoms with Mg atoms in the primitive calcite cell. For instance, one of the 12 Ca atoms in a 60-atom cell of calcite was substituted by one Mg atom to make a Mg/(Mg + Ca) of 1/12. Because the initial carbonate structures with Mg/(Mg + Ca) of 2/6, 3/6, and 4/6 have more than one configurations, all nonequivalent configurations in a 30-atom cell were calculated and the configurations with the lowest total energy were selected for dynamical matrices calculations. To test the effect of the supercell size, we also consider the structure with Mg/(Mg + Ca) of 2/12 in a 60-atom supercell, which is twice as large as that with Mg/(Mg + Ca) of 1/6 in a 30-atom supercell. The configuration with the lowest total energy among all nonequivalent configurations was selected as for dynamical matrices calculations. The optimized crystal structures of carbonates with variable Mg/(Mg + Ca) are shown in Fig. 1 with emphasis on Mg–O and Ca–O polyhedrons. Although the initial structures of carbonates with Mg/(Mg + Ca) of 3/6 and 1 are calcite-type structures, their optimized structures are consistent with dolomite and magnesite structures, respectively, as indicated by the fractional coordinates shown in Table S2. Both Ca and Mg have a coordination number (CN) of six in all calcite-type carbonates with variable Mg/(Mg + Ca), while Ca is ninefold coordinated in aragonite.

The calculated crystal lattice parameters of all carbonate minerals (Table S3), are consistent with experimental results within 1% (Fig. 2) after considering the temperature effect estimated using the volume expansion of calcite from static condition to 300 K, in which the volume of calcite increases by 1.8%. After the temperature correction, the crystal volumes are consistent with experimental data within 1%, indicating that the predicted crystal volumes in this study are reliable. The calculated vibrational frequencies of calcite, dolomite, magnesite, and aragonite agree well with experimental results (Fig. 3 and Table S4), with the slope between calculated frequencies and measured frequencies being 0.998 ± 0.020 (1σ, $R^2 = 0.9998$) (Fig. 3 and Table S4). This demonstrates that the calculated equilibrium isotope fractionation factors are reliable and accurate. Therefore, the LDA is a good exchange correlation functional for calculations of isotope fractionation among minerals, as demonstrated by previous studies (e.g., Li et al., 2011; Huang et al., 2013; Feng et al., 2014; Wu et al., 2015). Based on the analysis in previous work (Méheut et al., 2009), a deviation of n% on phonon frequencies would induce an error of n% at low temperature and 2n% at high temperature on $10^3 \ln \beta$. Therefore, the rel-

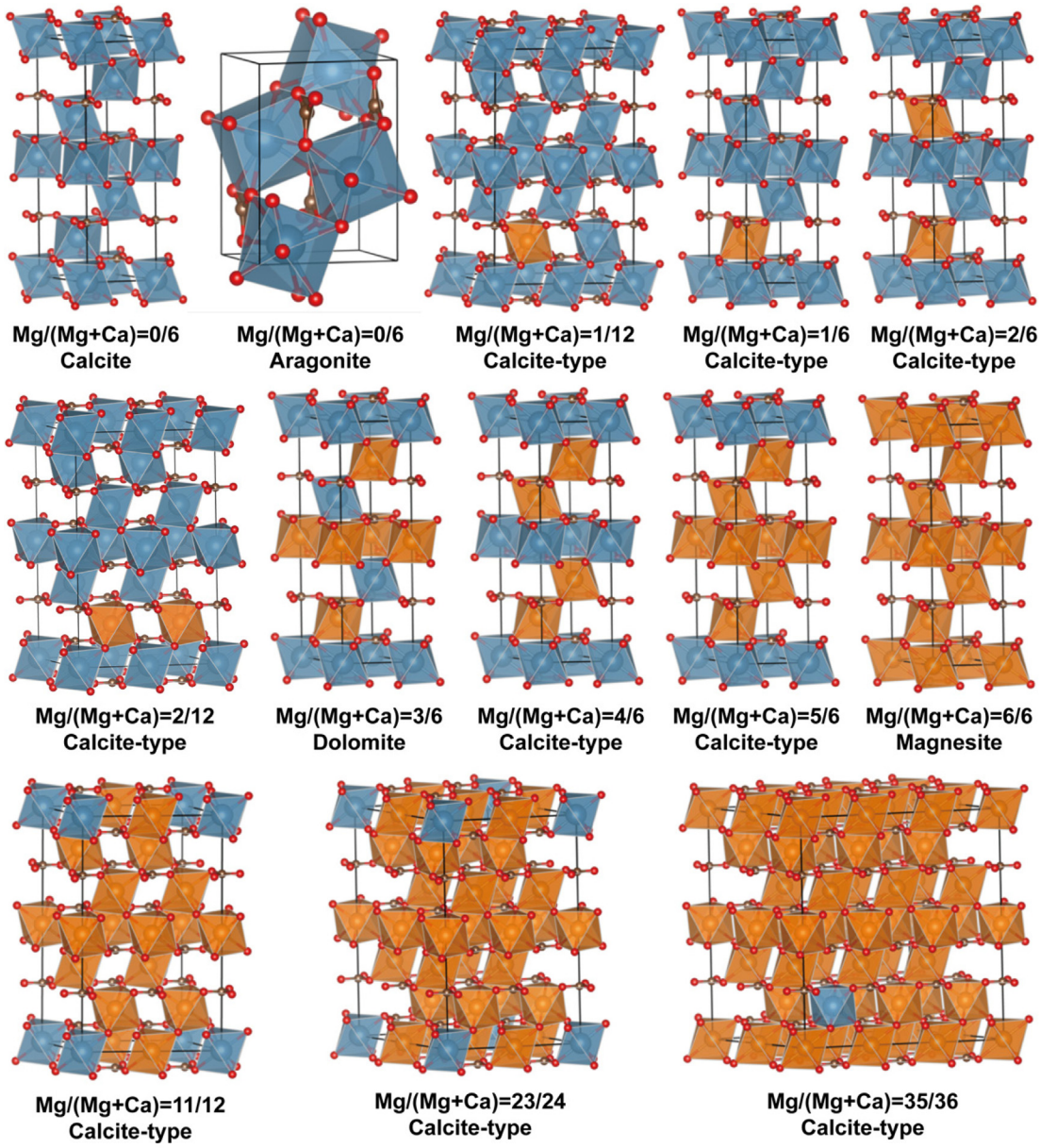

Fig. 1. Carbonate crystal structures with variable Mg/(Mg + Ca) with emphasis on Mg–O and Ca–O polyhedrons. Mg atoms are brown, Ca atoms cyan, C atoms dark brown, and O atoms red. All of these crystal structures are drawn using the software "VESTA" (Momma and Izumi, 2008). (For interpretation of the references to colour in this figure legend, the reader is referred to the web version of this article.)

ative uncertainties of our calculated $10^3 \ln \beta$ and $10^3 \ln \alpha$ are estimated at about 4% and 6%, respectively, under investigated temperature intervals (Méheut et al., 2009; Kowalski et al., 2013; Feng et al., 2014).

3.2. Average Mg–O and Ca–O bond lengths in carbonates

Average Mg–O and Ca–O bond lengths in carbonate minerals with variable Mg/(Mg + Ca) at static condition are reported in Table 1 and Fig. 4. As shown in Fig. 4, average Mg–O and Ca–O bond lengths vary with Mg/(Mg + Ca) of carbonate minerals. Our results show that average Mg–O and Ca–O bond lengths of the carbonate mineral with Mg/(Mg + Ca) of 1/6 calculated from the 60-atom supercell are consistent to those obtained from the 30-atom system. Dolomite has the shortest average Mg–O bond length and the longest average Ca–O bond length among all calculated carbonate minerals (Fig. 4a and b). Because the size of Ca^{2+} is larger than Mg^{2+} in carbonates, we expect that the Mg–O bond in calcite is longer than that in magnesite. Therefore, the average Mg–O bond length increases in the order of dolomite < magnesite < calcite. For the same taken, when Ca occupies the small Mg site in magnesite, Ca–O bond in magnesite is shorter than the one in calcite and thus the sequence of average Ca–O bond length is dolomite > calcite > magnesite. The predicted dif-

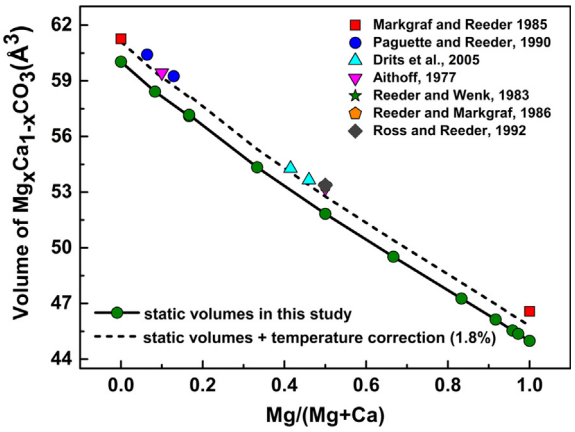

Fig. 2. The volumes of carbonate minerals $Mg_xCa_{1-x}CO_3$ versus x (Mg/(Mg + Ca)) at static condition. The black solid line shows that static volumes vary with Mg/(Mg + Ca). In order to correct the temperature effect, these volumes at ambient condition were estimated using calculated expansion volume of calcite at 300 K, which increases by 1.8% compared to the static volume of calcite (Table S3), as shown by the dash line. The relative difference between black dash line and experimental data is less than 1% (Althoff, 1977; Reeder and Wenk, 1983; Markgraf and Reeder, 1985; Reeder and Markgraf, 1986; Paquette and Reeder, 1990; Ross and Reeder, 1992; Drits et al., 2005).

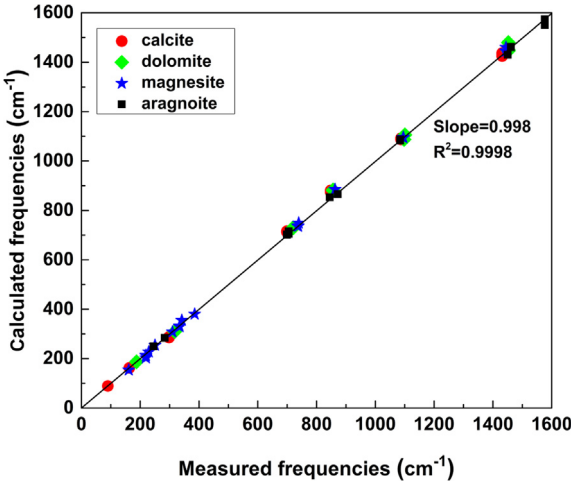

Fig. 3. Calculated frequencies of calcite, dolomite, magnesite and aragonite are compared to measured frequencies (more details in Table S4). Experimental data: Gunasekaran et al. (2006), Weir and Lippincott (1961), Hellwege et al. (1970), Gillet (1993), Grzechnik et al. (1999), Urmos et al. (1991).

ferences of average Mg–O bond length between dolomite and magnesite and average Ca–O bond length between dolomite and calcite from our calculations are −0.019 Å and 0.02 Å respectively (Table 1), which are consistent with the results from previous experimental and theoretical studies (Markgraf and Reeder, 1985; Reeder and Markgraf, 1986; Schauble, 2011). Finally, aragonite has an average Ca–O bond length much larger than calcite-type carbonate minerals (Table 1).

3.3. Isotope fractionation factors

The calculated reduced partition function ratios of $^{26}Mg/^{24}Mg$ ($10^3 \ln \beta_{^{26}Mg-^{24}Mg}$) and $^{44}Ca/^{40}Ca$ ($10^3 \ln \beta_{^{44}Ca-^{40}Ca}$) are shown in Fig. 5. The polynomial fitting parameters are reported in Table 2. $10^3 \ln \alpha_{minerals\text{-}dolomite}$ (equilibrium isotope fractionation factors between $Mg_xCa_{1-x}CO_3$ and dolomite) of $^{26}Mg/^{24}Mg$ and $^{44}Ca/^{40}Ca$ are plotted as a function of temperature in Fig. 6. Relative polynomial fitting parameters are given in Table 3. Small differences between results of calcite-type carbonate minerals with Mg/(Mg + Ca) of 1/6 and 2/12 indicate that the effect of supercell size is secondary and negligible. $10^3 \ln \beta_{^{26}Mg-^{24}Mg}$ increases in the order of Mg-calcite ($Mg_{1/12}Ca_{11/12}CO_3$) < magnesite < dolomite, which is generally consistent with previous theoretical results (Rustad et al., 2010; Schauble, 2011), as well as experimental and natural observations (Li et al., 2012, 2015; Saulnier et al., 2012; Mavromatis et al., 2013; Saenger and Wang, 2014). As expected from the compositional dependence of average bond lengths on Mg/(Mg + Ca), $10^3 \ln \beta_{^{26}Mg-^{24}Mg}$ and $10^3 \ln \beta_{^{44}Ca-^{40}Ca}$ of calcite-type carbonate minerals vary significantly with Mg/(Mg + Ca) (Figs. 5–7). The more sensitive the bond lengths to Mg/(Mg + Ca), the more rapidly the reduced partition function ratios change with Mg/(Mg + Ca). The $10^3 \ln \beta_{^{26}Mg-^{24}Mg}$ of dolomite (Mg/Ca = 1) is always higher than that of other calcite-type carbonate minerals with variable Mg proportions, while the $10^3 \ln \beta_{^{44}Ca-^{40}Ca}$ of dolomite is always lower than that of other calcite-type carbonates and higher than that of aragonite (Fig. 6), consistent with the fact that dolomite has the shortest Mg–O and the longest Ca–O bond length among all carbonate minerals. Notably, isotope fractionation factors change dramatically with Mg/(Mg + Ca). For example, at 300 K, $10^3 \ln \alpha$ of $^{26}Mg/^{24}Mg$ between calcites and dolomite range from −4.3‰ to 0 and $^{44}Ca/^{40}Ca$ from 0 to ~6‰ when Mg/(Mg + Ca) varies from 1/12 to 1/2. Therefore, in addition to temperature, Mg/(Mg + Ca) in carbonate minerals also significantly affects equilibrium isotope fractionation.

4. DISCUSSION

4.1. Concentration effect on average Ca–O and Mg–O bond lengths in carbonates

Based on first-principles calculation, Feng et al. (2014) found that Ca–O bond length in opx is highly sensitive to its Ca concentration. Our results show that average Ca–O and Mg–O bond lengths in the carbonate minerals are also significantly affected by their Mg contents (Table 1 and Fig. 4), suggesting that the concentration effect on bond length should be a ubiquitous phenomenon in minerals. When Element A replaces Element B with a different radius, Element A should be adapted to the mineral structure controlled by Element B. The effect from Element B increases with decreasing concentration of Element A. However, when the concentration of Element A is low enough, the

Table 1
Average Mg–O and Ca–O bond lengths in carbonates at static condition.

Minerals	Mg/(Mg + Ca)	Average bond length (Å)			
		Mg–O	Exp.	Ca–O	Exp.
Calcite-type	0			2.341	2.360[a]
	1/12	2.093		2.341	
	1/6	2.074		2.343	
	2/12	2.075		2.343	
	2/6	2.061		2.350	
	3/6	2.057	2.082[b]	2.361	2.381[b]
	4/6	2.073		2.351	
	5/6	2.078		2.336	
	11/12	2.082		2.292	
	23/24	2.080		2.274	
	35/36	2.079		2.273	
	6/6	2.076	2.102[a]		
Aragonite	6/6			2.491	2.529[*]

Experimental results:
[a] Markgraf and Reeder (1985).
[b] Reeder and Markgraf (1986).
[*] Antao and Hassan (2009).

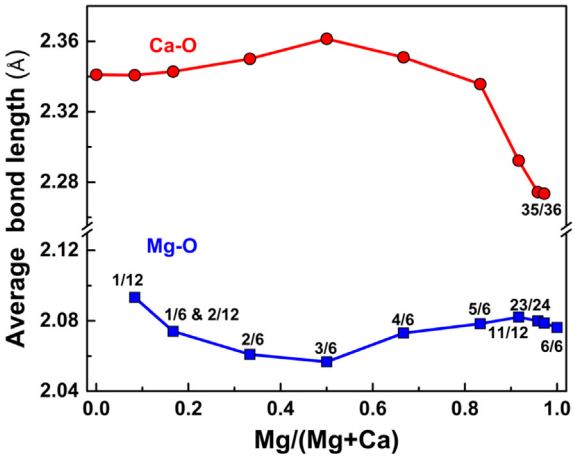

Fig. 4. Average (a) Mg–O bond and (b) Ca–O bond length of carbonate minerals versus Mg/(Mg + Ca).

effect from Element B should be saturated and A–O bond lengths will be close to a constant. On the other hand, with increasing concentration of Element A, average A–O bond length may gradually shift to a value similar to that of an A-dominated mineral, in which case the effect of Element B is small. This explains why average Mg–O bond length decreases with increasing Mg content from Mg-doped calcite to dolomite (Fig. 4a), and average Ca–O bond length increases with increasing Ca content from Ca-doped magnesite to dolomite (Fig. 4b).

Dolomite has symmetry-equivalent Mg and Ca sites. When Mg/(Mg + Ca) varies from 1/2 to 11/12, Mg–O bond length increases with increasing Mg/(Mg + Ca) because Mg atoms begin to occupy the larger Ca sites, resulting in much longer Mg–O bonds than the case in Mg sites. The average Mg–O bond length increases as more Mg atoms occupy the large Ca sites. Similarly, when Mg/(Mg + Ca) is less than 0.5, Ca–O bond length decreases with decreasing Mg/(Mg + Ca) because Ca atoms begin to occupy the smaller Mg sites, resulting in much shorter Ca–O bonds. This explains why average Mg–O bond length increases when Mg/(Mg + Ca) varies from 1/2 to 11/12 (Fig. 4a), and average Ca–O bond length decreases with increasing Ca content from dolomite to Mg-doped calcite (Fig. 4b). As a consequence, dolomite has the shortest average Mg–O and the longest average Ca–O bond lengths among carbonate minerals (Fig. 4a and b). This structure feature of carbonate minerals produces continuous variations of the Mg–O and Ca–O bond lengths from calcite to magnesite. This is different from the case of opx where Ca–O bond lengths vary with opx Ca concentration only when it is low enough (Feng et al., 2014).

4.2. Concentration effect on isotope fractionation factors

The equilibrium fractionation factors of Mg and Ca isotopes between calcite-type carbonate minerals (calcite-magnesite series) and dolomite vary significantly with Mg content in carbonate minerals. They are correlated with the average bond lengths with slightly different slopes for carbonate minerals with Mg/(Mg + Ca) < 1/2 and Mg/(Mg + Ca) > 1/2 (Fig. 8), which likely reflects the different dependences of average bond lengths on Mg/(Mg + Ca) due to the subtle disparity in structures between these two groups. When Mg/(Mg + Ca) < 1/2, Ca atoms are dominant relative to Mg atoms and show the major effect on structures. Similarly, Mg shows the major effect in carbonates when Mg/(Mg + Ca) > 1/2. Feng et al. (2014) also found that fractionation factors between opx and cpx are linearly correlated with average Ca–O bond lengths in opx. Equilibrium isotope fractionations are controlled by relevant bond strengths (Bigeleisen and Mayer, 1947; Urey, 1947). As analyzed in previous studies (Urey, 1947; Schauble et al., 2004; Hill and Schauble, 2008; Young et al., 2009), shorter chemical bonds correspond to stronger bond strengths and higher vibrational frequencies, leading

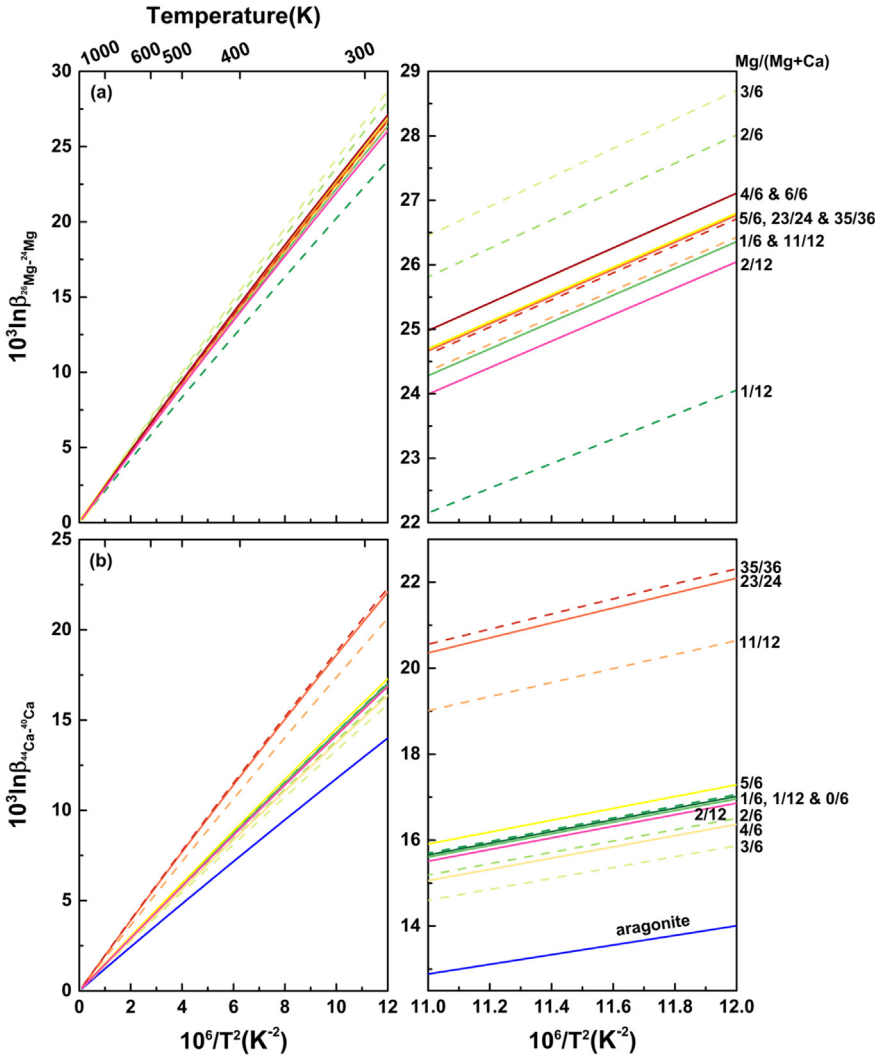

Fig. 5. (a) Mg isotope β-factors of calcite-type carbonate minerals, and (b) Ca isotope β-factors of calcite-type carbonate minerals and aragonite as a function of temperatures.

to enrichments in heavy isotopes relative to the longer and weaker chemical bonds. CN could also affect the bond strengths; however, the CNs of Ca and Mg in all calcite-type carbonates are six. Therefore, the bond lengths in calcite-type carbonate minerals dominantly control their bond strengths, resulting in a linear correlation between the inter-mineral isotope fractionations and the average bond lengths of carbonate minerals. This is similar to the case in opx and cpx where Ca is six-fold coordinated, and Ca isotopic fractionation between opx and cpx is also linearly correlated with Ca–O bond length in opx (Feng et al., 2014).

Pinilla et al. (2015) recently calculated equilibrium Mg isotopes fractionation factor between Mg-calcites with different Mg contents using the DFT method and they found that the calcite-type carbonate mineral with lesser Mg (3.12 mol%) is enriched in heavy Mg isotopes relative to the one with more Mg (6.25 mol%), which is in contrast with the expectation from this study that considers the carbonate minerals with Mg content higher than 6.25 mol %. The discrepancy probably arises from the difference in the calculation method. In their calculations, the cell parameters of carbonate minerals are fixed. Therefore, carbonate mineral with 3.12 mol% Mg must be under a higher pressure than the one with 6.25 mol% given that Mg atom is much smaller than Ca atom. Because increase of pressure can dramatically increase $10^3\ln\beta$ (Huang et al., 2013, 2014; Wu et al., 2015), this impractical pressure difference probably significantly increases $10^3\ln\beta$ of $^{26}Mg/^{24}Mg$ of the carbonate mineral with 3.12 mol% Mg relative to the one with 6.25 mol% Mg.

4.3. Implications for Mg and Ca isotopic compositions of carbonates

Stable isotopic compositions of carbonates provide important records on many low temperature geochemical processes. Their isotopic compositions are indispensable

Table 2
Polynomial fitting parameters of the calculated reduced partition function ratios ($10^3 \ln \beta$) of $^{26}Mg/^{24}Mg$ and $^{44}Ca/^{40}Ca$ for calcite-type carbonate minerals with variable Mg/(Mg + Ca) and aragonite.

Element	Minerals	Mg/(Mg + Ca)	a	b	c
$^{26}Mg/^{24}Mg$	Calcite-type	1/12	2.13577	−0.01317	1.91E−04
		1/6	2.34829	−0.01509	2.07E−04
		2/12	2.32144	−0.01485	1.89E−04
		2/6	2.50481	−0.01689	2.29E−04
		3/6	2.57088	−0.01774	2.40E−04
		4/6	2.42347	−0.01649	2.34E−04
		5/6	2.39560	−0.01643	2.40E−04
		11/12	2.36599	−0.01654	2.46E−04
		23/24	2.39509	−0.01657	2.42E−04
		35/36	2.39067	−0.01661	2.45E−04
		6/6	2.42674	−0.01688	2.48E−04
$^{44}Ca/^{40}Ca$	Aragonite	0/6	1.23384	−0.00749	1.66E−04
	Calcite-type	0/6	1.49037	−0.00729	1.07E−04
		1/12	1.49703	−0.00758	1.12E−04
		1/6	1.48731	−0.00748	1.11E−04
		2/12	1.47687	−0.00710	0.93E−04
		2/6	1.44802	−0.00737	1.13E−04
		3/6	1.39204	−0.00715	1.15E−04
		4/6	1.43798	−0.00762	1.21E−04
		5/6	1.52317	−0.00839	1.30E−04
		11/12	1.83571	−0.01157	1.65E−04
		23/24	1.97478	−0.01331	1.85E−04
		35/36	1.99278	−0.01331	1.87E−04

$10^3 \ln \beta = ax + bx^2 + cx^3$, where $x = 10^6/T^2$. T is temperature in Kelvin. All polynomial fittings are performed between 273 K to 2500 K.

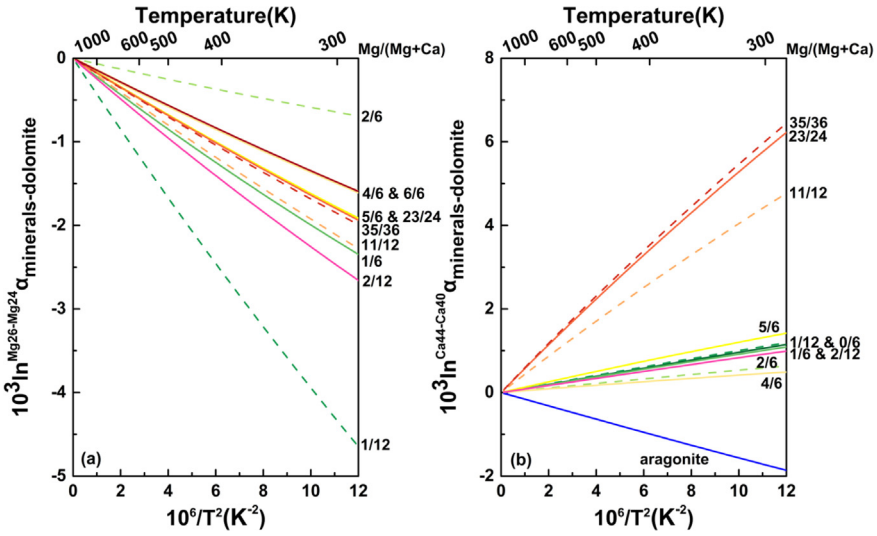

Fig. 6. Temperature dependence of the $10^3 \ln \alpha_{minerals\text{-}dolomite}$ of (a) Mg isotopes and (b) Ca isotopes. Calcite-type carbonate minerals are always enriched in lighter Mg isotopes and heavier Ca isotopes relative to dolomite. Aragonite is enriched in light Ca isotopes relative to calcite-type carbonate minerals.

for understanding these processes. $\delta^{26/24}Mg$ values of precipitated marine Mg-calcites vary from −5‰ to −1‰ (Galy et al., 2002; de Villiers et al., 2005; Tipper et al., 2006a,b; Buhl et al., 2007; Hippler et al., 2009) and $\delta^{26/24}Mg$ values of dolomites range from about −2‰ to −1‰ (Galy et al., 2002; Chang et al., 2003; Jacobson et al., 2010). These $\delta^{26/24}Mg$ variations of Mg-calcite (~4‰) and dolomite (~1‰) are ascribed to kinetic effects (Immenhauser et al., 2010) or unconfirmed "vital effects" (Chang et al., 2004). According to our calculated results, although kinetic effects are potentially important, the concentration effect on Mg and Ca isotope fractionation should be also considered. The variation of $10^3 \ln \alpha$ of Mg isotopes between Mg-calcite and dolomite caused by the difference

Table 3
Polynomial fitting parameters of $10^3 \ln \alpha_{minerals\text{-}dolomite}$ of $^{26}Mg/^{24}Mg$ and $^{44}Ca/^{40}Ca$. Minerals include calcite-type carbonate minerals with variable Mg/(Mg + Ca) and aragonite.

Element	Minerals	Mg/(Mg + Ca)	a	b	c
$^{26}Mg/^{24}Mg$	Calcite-type	1/12	−0.43511	4.6E−03	−4.9E−05
		1/6	−0.22259	2.7E−03	−3.3E−05
		2/12	−0.24944	2.9E−03	−5.1E−05
		2/6	−0.06607	8.5E−04	−1.1E−05
		4/6	−0.14741	1.3E−03	−6.0E−06
		5/6	−0.17528	1.3E−03	0.0
		11/12	−0.20489	1.2E−03	6.0E−06
		23/24	−0.17579	1.2E−03	2.0E−06
		35/36	−0.18021	1.1E−03	5.0E−06
		6/6	−0.14414	8.6E−04	8.0E−06
$^{44}Ca/^{40}Ca$	Aragonite	0/6	−0.15820	−3.4E−04	5.1E−05
	Calcite-type	0/6	0.09833	−1.4E−04	−8.0E−06
		1/12	0.10499	−4.3E−04	−3.0E−06
		1/6	0.09527	−3.3E−04	−4.0E−06
		2/12	0.08483	5.0E−05	−2.2E−05
		2/6	0.05598	−2.2E−04	−2.0E−06
		4/6	0.04594	−4.7E−04	6.0E−06
		5/6	0.13113	−1.2E−03	1.5E−05
		11/12	0.44367	−4.4E−03	5.0E−05
		23/24	0.58274	−6.2E−03	7.0E−05
		35/36	0.60074	−6.2E−03	7.2E−05

$10^3 \ln \alpha_{minerals\text{-}dolomite} = ax + bx^2 + cx^3$, where $x = 10^6/T^2$. T is temperature in Kelvin. All polynomial fittings are performed between 273 K to 2500 K.

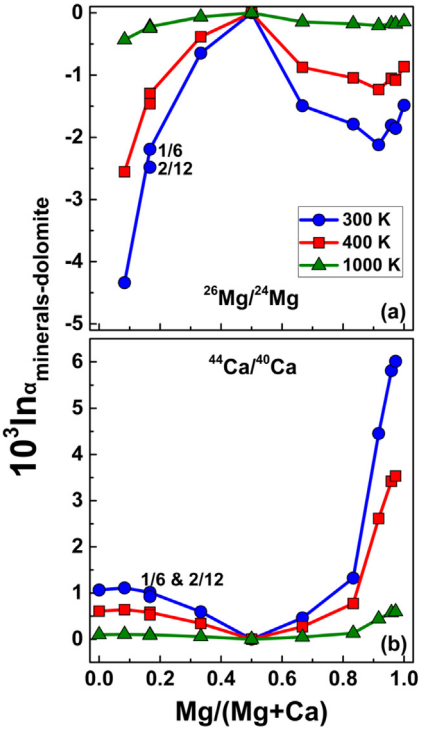

Fig. 7. $10^3 \ln \alpha_{minerals\text{-}dolomite}$ of (a) $^{26}Mg/^{24}Mg$ and (b) $^{44}Ca/^{40}Ca$ vary with Mg/(Mg + Ca) in calcite-type carbonate minerals.

of Mg content could be up to 4‰, and a small change of Mg/(Mg + Ca) in dolomite from *0.5* to *0.6* could account for 1‰ variation in $10^3 \ln \alpha$ at 300 K (Fig. 7). Furthermore, the concentration effect may play an important role in controlling Mg isotope fractionation during carbonates precipitation. Li et al. (2012) measured the Mg isotope fractionation between aqueous solution and Mg-bearing calcite with Mg/(Mg + Ca) ranging from 0.008 to 0.149. According to our calculated results, $10^3 \ln \alpha$ of $^{26}Mg/^{24}Mg$ between $Mg_{1/12}Ca_{11/12}CO_3$ and $Mg_{1/6}Ca_{5/6}CO_3$ is up to −2.1‰. Therefore, beyond the possible kinetic effect during the experiments, further research on concentration effect is also needed to understand this discrepancy.

Ca isotopic compositions of limestone and dolomite were reported in previous studies (Kasemann et al., 2005; Steuber and Buhl, 2006; Jacobson and Holmden, 2008; Holmden, 2009). A large offset of $\delta^{44/40}Ca$ between dolomite (−1.66‰) and limestone (−1.05‰) was observed, which shows a negative linear correlation with Mg/(Mg + Ca) ranging from 0 to 0.474 (Holmden, 2009). Based on our calculated results in Fig. 7b, the observed $\delta^{44/40}Ca$ difference (0.6‰) between limestone and dolomite may be related to the concentration effect on inter-mineral isotopic fractionation between $Mg_{1/12}Ca_{11/12}CO_3$ and dolomite at low temperature (Fig. 7b).

Finally, Ca and Mg isotopic compositions in marine carbonates have been used to constrain geochemical processes related to paleo-oceanography. For example, $\delta^{44/40}Ca$ variations of marine carbonates are used to infer the changes of global Ca cycling (De La Rocha, 2000; Heuser et al., 2005), and a simply steady-state model of Mg isotopes was used to constrain the oceanic cycling of Mg (Tipper et al., 2006b; Li et al., 2015). Because of the large concentration effects on equilibrium Mg and Ca isotopic fractionation among carbonate minerals, cautions need to be exercised in future studies.

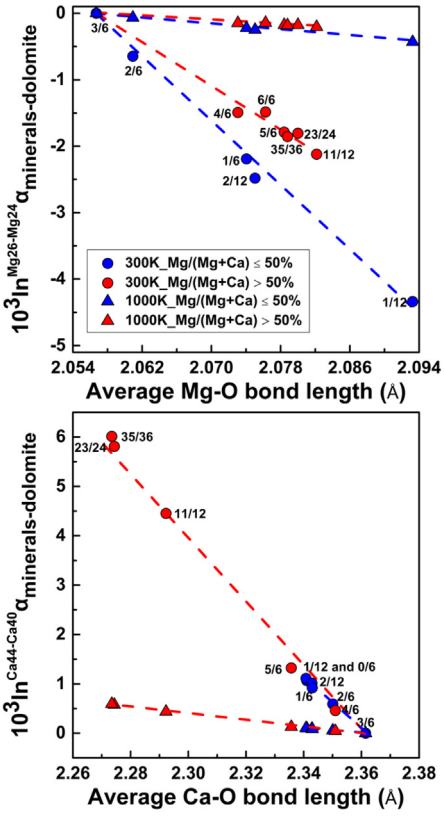

Fig. 8. The negative correlations between $10^3 \ln \alpha_{minerals\text{-}dolomite}$ of Mg and Ca isotopes and relative average Mg–O and Ca–O at 300 K and 1000 K, respectively. Shorter bonds are always enriched in heavy isotopes.

5. CONCLUSIONS

Our DFT calculations reveal that Ca–O and Mg–O bond lengths in carbonates are sensitive to their Mg and Ca contents. Mg–O bond length decreases rapidly with increasing Mg/(Mg + Ca) when Mg/(Mg + Ca) < 1/2. However, when Mg/(Mg + Ca) > 1/2, Mg–O bond length increases with increasing Mg/(Mg + Ca), because Mg atoms begin to occupy the Ca sites of dolomite, which results in much longer Mg–O bond length than Mg atoms in Mg sites of dolomite. Ca–O bond length increases slightly with increasing Mg/(Mg + Ca) when Mg/(Mg + Ca) < 1/2, then it decreases with increasing Mg/(Mg + Ca) when Mg/(Mg + Ca) > 1/2, with dolomite having the longest Ca–O bond and the shortest Mg–O bond lengths among carbonate minerals. Such concentration effect on Ca–O bond length is most prominent when Ca/(Mg + Ca) < 1/6.

The calculated equilibrium fractionation factors of Mg-Ca isotopes among carbonate minerals ($Mg_xCa_{1-x}CO_3$) are linearly correlated with their average bond lengths. Mg/(Mg + Ca) significantly affects Mg and Ca isotope fractionations among carbonates. Dolomite (Mg/Ca = 1) is enriched in heavy Mg isotopes but depleted in heavy Ca isotopes relative to other carbonate minerals. At 300 K, the equilibrium fractionation of Mg isotopes between Mg-calcite with various Mg/(Mg + Ca) and dolomite can be up to 4‰, comparable to the observed range of $\delta^{26/24}$Mg in marine Mg-calcite. A small change of Mg/(Mg + Ca) in dolomite from *0.5* to *0.6* could produce 1‰ variation in $\delta^{26/24}$Mg at 300 K. Therefore, the concentration effect in carbonate minerals should be taken into account when applying the isotope fractionation coefficients to understand geochemical processes.

ACKNOWLEDGMENTS

This work is financially supported by Natural Science Foundation of China (41325011, 41473011, 41090370), 111 Project, and Special Program for Applied Research on Super Computation of the NSFC-Guangdong Joint Fund. Shichun Huang acknowledges support from NSF grant EAR-1524387. The computations were conducted partly in Supercomputing Center of the University of Science and Technology of China. We are grateful to the constructive comments from three anonymous reviewers and editorial handling by Andrew Jacobson.

APPENDIX A. SUPPLEMENTARY MATERIAL

Supplementary data associated with this article can be found, in the online version, at http://dx.doi.org/10.1016/j.gca.2017.03.023.

REFERENCES

Ader M., Macouin M., Trindade R. I. F., Hadrien M.-H., Yang Z., Sun Z. and Besse J. (2009) A multilayered water column in the Ediacaran Yangtze platform? Insights from carbonate and organic matter paired δ^{13}C. *Earth Planet. Sci. Lett.* **288**, 213–227.

Althoff P. L. (1977) Structural refinements of dolomite and a magnesian calcite and implications for dolomite formation in the marine environment. *Am. Mineral.* **62**, 772–783.

Antao S. M. and Hassan I. (2009) The orthorhombic structure of $CaCO_3$, $SrCO_3$, $PbCO_3$ and $BaCO_3$: linear structural trends. *Can. Mineral.* **47**, 1245–1255.

Bemis B. E., Spero H. J., Bijma J. and Lea D. W. (1998) Reevaluation of the oxygen isotopic composition of planktonic foraminifera: experimental results and revised paleotemperature equations. *Paleoceanography* **13**, 150–160.

Bigeleisen J. and Mayer M. G. (1947) Calculation of equilibrium constants for isotopic exchange reactions. *J. Chem. Phys.* **15**, 261.

Buhl D., Immenhauser A., Smeulders G., Kabiri L. and Richter D. K. (2007) Time series δ^{26}Mg analysis in speleothem calcite: kinetic versus equilibrium fractionation, comparison with other proxies and implications for palaeoclimate research. *Chem. Geol.* **244**, 715–729.

Chang V. T.-C., Makishima A., Belshaw N. S. and O'Nions R. K. (2003) Purification of Mg from low-Mg biogenic carbonates for isotope ratio determination using multiple collector ICP-MS. *J. Anal. At. Spectrom.* **18**, 296–301.

Chang V. T. C., Williams R. J. P., Makishima A., Belshawl N. S. and O'Nions R. K. (2004) Mg and Ca isotope fractionation during $CaCO_3$ biomineralisation. *Biochem. Biophys. Res. Commun.* **323**, 79–85.

Cheng Z., Zhang Z., Hou T., Santosh M., Zhang D. and Ke S. (2015) Petrogenesis of nephelinites from the Tarim Large Igneous Province, NW China: implications for mantle source

characteristics and plume–lithosphere interaction. *Lithos* **220–223**, 164–178.

DePaolo D. J. (2004) Calcium isotopic variations produced by biological, kinetic, radiogenic and nucleosynthetic processes. *Rev. Mineral. Geochem.* **55**, 255–288.

Drits V. A., McCarty D. K., Sakharov B. and Milliken K. L. (2005) New insight into structural and compositional variability in some ancient excess-Ca dolomite. *Can. Mineral.* **43**, 1255–1290.

Farkaš J., Buhl D., Blenkinsop J. and Veizer J. (2007) Evolution of the oceanic calcium cycle during the late Mesozoic: evidence from $\delta^{44/40}$Ca of marine skeletal carbonates. *Earth Planet. Sci. Lett.* **253**, 96–111.

Feng C., Qin T., Huang S., Wu Z. and Huang F. (2014) First-principles investigations of equilibrium calcium isotope fractionation between clinopyroxene and Ca-doped orthopyroxene. *Geochim. Cosmochim. Acta* **143**, 132–142.

Galy A., Bar-Matthews M., Halicz L. and O'Nions R. K. (2002) Mg isotopic composition of carbonate: insight from speleothem formation. *Earth Planet. Sci. Lett.* **201**, 105–115.

Giannozzi P., Baroni S., Bonini N., Calandra M., Car R., Cavazzoni C., Ceresoli D., Chiarotti G. L., Cococcioni M., Dabo I., Dal Corso A., de Gironcoli S., Fabris S., Fratesi G., Gebauer R., Gerstmann U., Gougoussis C., Kokalj A., Lazzeri M., Martin-Samos L., Marzari N., Mauri F., Mazzarello R., Paolini S., Pasquarello A., Paulatto L., Sbraccia C., Scandolo S., Sclauzero G., Seitsonen A. P., Smogunov A., Umari P. and Wentzcovitch R. M. (2009) QUANTUM ESPRESSO: a modular and open-source software project for quantum simulations of materials. *J. Phys. Condens. Matter* **21**, 395502.

Gillet P. (1993) Stability of magnesite ($MgCO_3$) at mantle pressure and temperature conditions; a Raman spectroscopic study. *Am. Mineral.* **78**, 1328–1331.

Graf D. L. (1961) Crystallographic tables for the rhombohedral carbonates. *Am. Mineral.* **46**, 1283–1316.

Griffith E. M., Schauble E. A., Bullen T. D. and Paytan A. (2008) Characterization of calcium isotopes in natural and synthetic barite. *Geochim. Cosmochim. Acta* **72**, 5641–5658.

Grzechnik A., Simon P., Gillet P. and McMillan P. (1999) An infrared study of $MgCO_3$ at high pressure. *Phys. B Condens. Matter* **262**, 67–73.

Gunasekaran S., Anbalagan G. and Pandi S. (2006) Raman and infrared spectra of carbonates of calcite structure. *J. Raman Spectrosc.* **37**, 892–899.

Hellwege K. H., Lesch W., Plihal M. and Schaack G. (1970) Zwei-Phononen-Absorptionsspektren und Dispersion der Schwingungszweige in Kristallen der Kalkspatstruktur. *Zeitschrift für Phys. A Hadron. Nucl.* **232**, 61–86.

Heuser A., Eisenhauer A., Böhm F., Wallmann K., Gussone N., Pearson P. N., Nägler T. F. and Dullo W.-C. (2005) Calcium isotope ($\delta^{44/40}$Ca) variations of Neogene planktonic foraminifera. *Paleoceanography* **20**, PA2013.

Higgins J. A. and Schrag D. P. (2010) Constraining magnesium cycling in marine sediments using magnesium isotopes. *Geochim. Cosmochim. Acta* **74**, 5039–5053.

Hill P. S. and Schauble E. A. (2008) Modeling the effects of bond environment on equilibrium iron isotope fractionation in ferric aquo-chloro complexes. *Geochim. Cosmochim. Acta* **72**, 1939–1958.

Hippler D., Buhl D., Witbaard R., Richter D. K. and Immenhauser A. (2009) Towards a better understanding of magnesium-isotope ratios from marine skeletal carbonates. *Geochim. Cosmochim. Acta* **73**, 6134–6146.

Hoffman P. F., Kaufman A. J., Halverson G. P. and Schrag D. P. (1998) A neoproterozoic snowball earth. *Science* **281**, 1342–1346.

Holmden C. (2009) Ca isotope study of Ordovician dolomite, limestone, and anhydrite in the Williston Basin: implications for subsurface dolomitization and local Ca cycling. *Chem. Geol.* **268**, 180–188.

Huang Y. and Fairchild I. J. (2001) Partitioning of Sr^{2+} and Mg^{2+} into calcite under karst-analogue experimental conditions. *Geochim. Cosmochim. Acta* **65**, 47–62.

Huang S., Farkaš J. and Jacobsen S. B. (2011) Stable calcium isotopic compositions of Hawaiian shield lavas: Evidence for recycling of ancient marine carbonates into the mantle. *Geochim. Cosmochim. Acta* **75**, 4987–4997.

Huang F., Chen L., Wu Z. and Wang W. (2013) First-principles calculations of equilibrium Mg isotope fractionations between garnet, clinopyroxene, orthopyroxene, and olivine: implications for Mg isotope thermometry. *Earth Planet. Sci. Lett.* **367**, 61–70.

Huang F., Wu Z., Huang S. and Wu F. (2014) First-principles calculations of equilibrium silicon isotope fractionation among mantle minerals. *Geochim. Cosmochim. Acta* **140**, 509–520.

Huang J., Li S.-G., Xiao Y., Ke S., Li W.-Y. and Tian Y. (2015) Origin of low δ^{26}Mg Cenozoic basalts from South China Block and their geodynamic implications. *Geochim. Cosmochim. Acta* **164**, 298–317.

Immenhauser A., Buhl D., Richter D., Niedermayr A., Riechelmann D., Dietzel M. and Schulte U. (2010) Magnesium-isotope fractionation during low-Mg calcite precipitation in a limestone cave – field study and experiments. *Geochim. Cosmochim. Acta* **74**, 4346–4364.

Jacobson A. D. and Holmden C. (2008) Δ^{44}Ca evolution in a carbonate aquifer and its bearing on the equilibrium isotope fractionation factor for calcite. *Earth Planet. Sci. Lett.* **270**, 349–353.

Jacobson A. D., Zhang Z., Lundstrom C. and Huang F. (2010) Behavior of Mg isotopes during dedolomitization in the Madison Aquifer, South Dakota. *Earth Planet. Sci. Lett.* **297**, 446–452.

Johnston D. T., Poulton S. W., Goldberg T., Sergeev V. N., Podkovyrov V., Vorob'eva N. G., Bekker A. and Knoll A. H. (2012) Late Ediacaran redox stability and metazoan evolution. *Earth Planet. Sci. Lett.* **335–336**, 25–35.

Kasemann S. A., Hawkesworth C. J., Prave A. R., Fallick A. E. and Pearson P. N. (2005) Boron and calcium isotope composition in Neoproterozoic carbonate rocks from Namibia: evidence for extreme environmental change. *Earth Planet. Sci. Lett.* **231**, 73–86.

Kaufman A. and Knoll A. (1995) Neoproterozoic variations in the C-isotopic composition of seawater: stratigraphic and biogeochemical implications. *Precambrian Res.* **73**, 27–49.

Kim S.-T. and O'Neil J. R. (1997) Equilibrium and nonequilibrium oxygen isotope effects in synthetic carbonates. *Geochim. Cosmochim. Acta* **61**, 3461–3475.

Kowalski P. M. and Jahn S. (2011) Prediction of equilibrium Li isotope fractionation between minerals and aqueous solutions at high P and T: an efficient ab initio approach. *Geochim. Cosmochim. Acta* **75**, 6112–6123.

Kowalski P. M., Wunder B. and Jahn S. (2013) Ab initio prediction of equilibrium boron isotope fractionation between minerals and aqueous fluids at high P and T. *Geochim. Cosmochim. Acta* **101**, 285–301.

De La Rocha C. L. (2000) Isotopic evidence for variations in the marine calcium cycle over the cenozoic. *Science* **289**, 1176–1178.

Land L. S. (1998) Failure to precipitate dolomite at 25 °C from dilute solution despite 1000-fold oversaturation after 32 years. *Aquat. Geochem.* **4**, 361–368.

Lea D. W. (2014) Elemental and isotopic proxies of past ocean temperatures. In *Treatise on Geochemistry*. Elsevier, pp. 373–397.

Lejaeghere K., Bihlmayer G., Bjorkman T., Blaha P., Blugel S., Blum V., Caliste D., Castelli I. E., Clark S. J., Dal Corso A., de Gironcoli S., Deutsch T., Dewhurst J. K., Di Marco I., Draxl C., Du ak M., Eriksson O., Flores-Livas J. A., Garrity K. F., Genovese L., Giannozzi P., Giantomassi M., Goedecker S., Gonze X., Granas O., Gross E. K. U., Gulans A., Gygi F., Hamann D. R., Hasnip P. J., Holzwarth N. A. W., Iu an D., Jochym D. B., Jollet F., Jones D., Kresse G., Koepernik K., Kucukbenli E., Kvashnin Y. O., Locht I. L. M., Lubeck S., Marsman M., Marzari N., Nitzsche U., Nordstrom L., Ozaki T., Paulatto L., Pickard C. J., Poelmans W., Probert M. I. J., Refson K., Richter M., Rignanese G.-M., Saha S., Scheffler M., Schlipf M., Schwarz K., Sharma S., Tavazza F., Thunstrom P., Tkatchenko A., Torrent M., Vanderbilt D., van Setten M. J., Van Speybroeck V., Wills J. M., Yates J. R., Zhang G.-X. and Cottenier S. (2016) Reproducibility in density functional theory calculations of solids. *Science* **351**, aad3000-aad3000.

Li X. and Liu Y. (2011) Equilibrium Se isotope fractionation parameters: a first-principles study. *Earth Planet. Sci. Lett.* **304**, 113–120.

Li W.-Y., Teng F.-Z., Xiao Y. and Huang J. (2011) High-temperature inter-mineral magnesium isotope fractionation in eclogite from the Dabie orogen, China. *Earth Planet. Sci. Lett.* **304**, 224–230.

Li W., Chakraborty S., Beard B. L., Romanek C. S. and Johnson C. M. (2012) Magnesium isotope fractionation during precipitation of inorganic calcite under laboratory conditions. *Earth Planet. Sci. Lett.* **333–334**, 304–316.

Li W., Beard B. L., Li C., Xu H. and Johnson C. M. (2015) Experimental calibration of Mg isotope fractionation between dolomite and aqueous solution and its geological implications. *Geochim. Cosmochim. Acta* **157**, 164–181.

Liu D., Zhao Z., Zhu D.-C., Niu Y., Widom E., Teng F.-Z., DePaolo D. J., Ke S., Xu J.-F., Wang Q. and Mo X. (2015) Identifying mantle carbonatite metasomatism through Os–Sr–Mg isotopes in Tibetan ultrapotassic rocks. *Earth Planet. Sci. Lett.* **430**, 458–469.

Markgraf S. and Reeder R. (1985) High-temperature structure refinements of calcite and magnesite. *Am. Miner.* **70**, 590–600.

Mavromatis V., Gautier Q., Bosc O. and Schott J. (2013) Kinetics of Mg partition and Mg stable isotope fractionation during its incorporation in calcite. *Geochim. Cosmochim. Acta* **114**, 188–203.

McDermott F. (2004) Palaeo-climate reconstruction from stable isotope variations in speleothems: a review. *Quat. Sci. Rev.* **23**, 901–918.

Méheut M., Lazzeri M., Balan E. and Mauri F. (2009) Structural control over equilibrium silicon and oxygen isotopic fractionation: a first-principles density-functional theory study. *Chem. Geol.* **258**, 28–37.

Meldrum F. C. and Hyde S. T. (2001) Morphological influence of magnesium and organic additives on the precipitation of calcite. *J. Cryst. Growth* **231**, 544–558.

Meyer K. M., Yu M., Lehrmann D., van de Schootbrugge B. and Payne J. L. (2013) Constraints on Early Triassic carbon cycle dynamics from paired organic and inorganic carbon isotope records. *Earth Planet. Sci. Lett.* **361**, 429–435.

Momma K. and Izumi F. (2008) VESTA : a three-dimensional visualization system for electronic and structural analysis. *J. Appl. Crystallogr.* **41**, 653–658.

Mucci A. and Morse J. W. (1983) The incorporation of Mg^{2+} and Sr^{2+} into calcite overgrowths: influences of growth rate and solution composition. *Geochim. Cosmochim. Acta* **47**, 217–233.

Mucci A. (1986) Growth kinetics and composition of magnesian calcite overgrowths precipitated from seawater: quantitative influence of orthophosphate ions. *Geochim. Cosmochim. Acta* **50**, 2255–2265.

Paquette J. and Reeder R. J. (1990) Single-crystal X-ray structure refinements of two biogenic magnesian calcite crystals. *Am. Mineral.* **75**, 1151–1158.

Pearce C. R., Saldi G. D., Schott J. and Oelkers E. H. (2012) Isotopic fractionation during congruent dissolution, precipitation and at equilibrium: evidence from Mg isotopes. *Geochim. Cosmochim. Acta* **92**, 170–183.

Perdew J. P. and Zunger A. (1981) Self-interaction correction to density-functional approximations for many-electron systems. *Phys. Rev. B* **23**, 5048–5079.

Pinilla C., Blanchard M., Balan E., Natarajan S. K., Vuilleumier R. and Mauri F. (2015) Equilibrium magnesium isotope fractionation between aqueous Mg2+ and carbonate minerals: insights from path integral molecular dynamics. *Geochim. Cosmochim. Acta* **163**, 126–139.

Reeder R. J. and Wenk H. R. (1983) Structure refinements of some thermally disordered dolomites. *Am. Mineral.* **68**, 769–776.

Reeder R. J. and Markgraf S. A. (1986) High-temperature crystal chemistry of dolomite. *Am. Mineral.* **7**, 795–804.

Richet P., Bottinga Y. and Javoy M. (1977) A review of hydrogen, carbon, nitrogen, oxygen, sulphur, and chlorine stable isotope fractionation among gaseous molecules. *Annu. Rev. Earth Planet. Sci.* **5**, 65–110.

Ross N. L. and Reeder R. J. (1992) High-pressure structural study of dolomite and ankerite. *Am. Mineral.* **77**, 412–421.

Rustad J. R., Casey W. H., Yin Q.-Z., Bylaska E. J., Felmy A. R., Bogatko S. A., Jackson V. E. and Dixon D. A. (2010) Isotopic fractionation of Mg^{2+}(aq), Ca^{2+}(aq), and Fe^{2+}(aq) with carbonate minerals. *Geochim. Cosmochim. Acta* **74**, 6301–6323.

Saenger C. and Wang Z. (2014) Magnesium isotope fractionation in biogenic and abiogenic carbonates: implications for paleoenvironmental proxies. *Quat. Sci. Rev.* **90**, 1–21.

Sahoo S. K., Planavsky N. J., Kendall B., Wang X., Shi X., Scott C., Anbar A. D., Lyons T. W. and Jiang G. (2012) Ocean oxygenation in the wake of the Marinoan glaciation. *Nature* **489**, 546–549.

Saulnier S., Rollion-Bard C., Vigier N. and Chaussidon M. (2012) Mg isotope fractionation during calcite precipitation: an experimental study. *Geochim. Cosmochim. Acta* **91**, 75–91.

Schauble E., Rossman G. R. and Taylor H. P. (2004) Theoretical estimates of equilibrium chromium-isotope fractionations. *Chem. Geol.* **205**, 99–114.

Schauble E. A. (2011) First-principles estimates of equilibrium magnesium isotope fractionation in silicate, oxide, carbonate and hexaaquamagnesium(2+) crystals. *Geochim. Cosmochim. Acta* **75**, 844–869.

Shields-Zhou G. and Och L. (2011) The case for a neoproterozoic oxygenation event: geochemical evidence and biological consequences. *GSA Today* **21**, 4–11.

Steuber T. and Buhl D. (2006) Calcium-isotope fractionation in selected modern and ancient marine carbonates. *Geochim. Cosmochim. Acta* **70**, 5507–5521.

Tesoriero A. J. and Pankow J. F. (1996) Solid solution partitioning of Sr^{2+}, Ba^{2+}, and Cd^{2+} to calcite. *Geochim. Cosmochim. Acta* **60**, 1053–1063.

Tipper E. T., Galy A. and Bickle M. J. (2006a) Riverine evidence for a fractionated reservoir of Ca and Mg on the continents: implications for the oceanic Ca cycle. *Earth Planet. Sci. Lett.* **247**, 267–279.

Tipper E. T., Galy A., Gaillardet J., Bickle M. J., Elderfield H. and Carder E. A. (2006b) The magnesium isotope budget of the

modern ocean: constraints from riverine magnesium isotope ratios. *Earth Planet. Sci. Lett.* **250**, 241–253.

Troullier N. and Martins J. L. (1991) Efficient pseudopotentials for plane-wave calculations. II. Operators for fast iterative diagonalization. *Phys. Rev. B* **43**, 8861–8869.

Urey, H.C., 1947. The thermodynamic properties of isotopic substances. In: Karato, S.-I. (Ed.), J. Chem. Soc., 562.

Urmos J., Sharma S. K. and Mackenzie F. T. (1991) Characterization of some biogenic carbonates with Raman spectroscopy. *Am. Mineral.* **76**, 641–646.

Vanderbilt D. (1990) Soft self-consistent pseudopotentials in a generalized eigenvalue formalism. *Phys. Rev. B* **41**, 7892–7895.

de Villiers S., Dickson J. A. D. and Ellam R. M. (2005) The composition of the continental river weathering flux deduced from seawater Mg isotopes. *Chem. Geol.* **216**, 133–142.

Warren J. (2000) Dolomite: occurence, evolution and economically important associations. *Earth Sci. Rev.* **52**, 1–81.

Weir C. E. and Lippincott E. R. (1961) Infrared studies of aragonite, calcite, and vaterite type structures in the borates, carbonates, and nitrates. *J. Res. Natl. Bur. Stand. Sect. A Phys. Chem.* **65A**, 173.

Wentzcovitch R. M. (1991) Invariant molecular-dynamics approach to structural phase transitions. *Phys. Rev. B* **44**, 2358–2361.

Wentzcovitch R. M., Yu Y. G. and Wu Z. (2010) Thermodynamic properties and phase relations in mantle minerals investigated by first principles quasiharmonic theory. *Rev. Mineral. Geochem.* **71**, 59–98.

Werne J. P. and Hollander D. J. (2004) Balancing supply and demand: controls on carbon isotope fractionation in the Cariaco Basin (Venezuela) Younger Dryas to present. *Mar. Chem.* **92**, 275–293.

Wu Z., Huang F. and Huang S. (2015) Isotope fractionation induced by phase transformation: first-principles investigation for Mg_2SiO_4. *Earth Planet. Sci. Lett.* **409**, 339–347.

Yang W., Teng F.-Z., Zhang H.-F. and Li S.-G. (2012) Magnesium isotopic systematics of continental basalts from the North China craton: implications for tracing subducted carbonate in the mantle. *Chem. Geol.* **328**, 185–194.

Young E. D., Tonui E., Manning C. E., Schauble E. and Macris C. A. (2009) Spinel–olivine magnesium isotope thermometry in the mantle and implications for the Mg isotopic composition of Earth. *Earth Planet. Sci. Lett.* **288**, 524–533.

Zenger D. H., Dunham J. B. and Ethington R. L. (1980). In *Concepts and Models of Dolomitization* (eds. D. H. Zenger, J. B. Dunham and R. L. Ethington). SEPM (Society for Sedimentary Geology).

Zhang H. and Li S. (2012) Deep carbon recycling and isotope tracing: review and prospect. *Sci. China Earth Sci.* **55**, 1929–1941.

Associate editor: Andrew D. Jacobson